Supplementary Figures

Figure S1.

Global levels of FOXO3 *O*-GlcNAcylation are increased in pancreatic cancer cell lines. **A,** Western blot analysis of *O*-GlcNAcylation in human pancreas cell lines (e.g., HPDE, PANC-1, BxPC-3, HPAC) (left panel) and the relative ratio of *O*-GlcNAc to GAPDH (normalization control; right panel). The global *O*-GlcNAc levels increased substantially in the pancreatic cancer cell line PANC-1 (4.00 ± 0.72-fold, $n = 3$) relative to the immortalized epithelial pancreas cell line HPDE. **B,** Immunoprecipitation and Western blotting (IP/WB) analysis of FOXO3 and *O*-GlcNAc levels in human pancreatic cell lines (left panel). The relative ratio of *O*-GlcNAc to FOXO3 (right panel). FOXO3 levels were also increased in PANC-1, BxPC-3, and HPAC cells, with higher relative ratios of *O*-GlcNAc to FOXO3 in PANC-1 and HPAC cell lines (1.56 ± 0.15-fold and 1.29 ± 0.2-fold, $n = 3$). Data from three independent experiments were quantified and are presented as averages. $^{**}p < 0.005$.

Figure S2.

Mass spectra of *O*-GlcNAc-modified peptides. Mass spectrometry (MS) data and tandem MS (MS/MS) peaks of *O*-GlcNAcylated FOXO3 peptides enriched from FOXO3-overexpressing FOX-OV cells (derived from PANC-1 cells). **A,** 741.34 MS spectra, 222.00937 from (741.34, 3+), and MS/MS fragmentation of DDSPSQLSKWPGSPTS RSS (S3 HexNAc) – S284; **B,** 860.39 MS spectra, 2579.15091 from (860.39, 3+), and MS/MS fragmentation of DDSPSQLSKWPGSPTSRSSDEL (S6 HexNAc) – S286; **C,** 610.79 MS spectra, 1220.56438 from (610.79, 2+), and MS/MS fragmentation of SSSFPYTTK (S1 HexNAc) – S411; **D,** 689.32 MS spectra, 1377.63481 from (689.32, 2+), and MS/MS fragmentation of DLLTSDSLSHS (T4 HexNAc) – T475; **E,** 791.36 MS spectra, 1580.71147 from (791.36, 2+), and MS/MS fragmentation of DLLTSDSLSHS (T4 HexNAc, S5 HexNAc) – T475, S476; **F,**

689.82 MS spectra, 1377.63530 from (689.82, 2+), and MS/MS fragmentation of DLLTSDSLSHS (S11 HexNAc) – S482; **G,** 1115.03 MS spectra, 2229.05498 from (1115.03, 2+), and MS/MS fragmentation of ALSNSVSNMGLSESSSLGS AK (S3 HexNAc) –S551.

Figure S3.

Establishment of FOXO3-overexpressing pancreatic cancer cell lines lacking *O*-GlcNAc or phosphoryl groups at seven different amino acids. Western blot analysis confirmed that the transfected *O*-GlcNAcylation and phosphorylation-deficient FOXO3-overexpressing pancreatic cancer cell line was ready to use. Mutant cell transfection was also confirmed by western blotting, which demonstrated readiness of the *O*-GlcNAcylation and phosphorylation-deficient FOXO3-overexpressing pancreatic cancer cell line.

Figure S4.

Experimental survey of changes in the expression of genes and proteins involved in pancreatic cancer cell proliferation and cell cycle. **A,** The expression levels of various cell cycle regulatory proteins (p53, p21, MDM2, OGT, OGA, CDK1, CDK2, CDK4, Cyclin A, Cyclin D1, Cyclin E, Cyclin G2 and GAPDH) in FOXO3 mutants were determined by western blotting. All data were quantified and are presented as the means ± standard deviations from three independent experiments. **B,** qRT-PCR analysis of genes encoding hexosamine biosynthetic pathway (HBP) proteins (OGT, OGA, PFK1, GFAT) in HPDE cells (normal-like pancreas cell line), PANC-1 cell, FOX-OV (containing *O*-GlcNAc at S284), and S284A mutant cell lines (lacking *O*-GlcNAc at S284). **C,** Western blot analysis of HBP proteins (OGT, OGA, PFK1, GFAT) in HPDE cells (normal-like pancreas cell line), PANC-1 cell, FOX-OV (containing *O*-GlcNAc at S284), and S284A mutant cell lines (lacking *O*-GlcNAc at S284). $*p < 0.001$, $**p < 0.005$. N.S., not significant for indicated comparison.

Figure S5.

Changes in *O*-GlcNAcylation at FOXO3 S284 did not appear to affect the transcriptional activity of p21. **A,** *O*-GlcNAcylation of S284 within FOXO3 is unlikely to correlate with FOXO3 localization. The nuclear fractionation of PANC-1 cells was confirmed by western blotting. **B,** Chromatin IP (ChIP) of FOXO3 with anti-FOXO3 antibody in diverse *O*-GlcNAc mutants of S284 within FOXO3. Data from three independent experiments were quantified and are presented as average values. ***$p < 0.0001$.

Figure S1

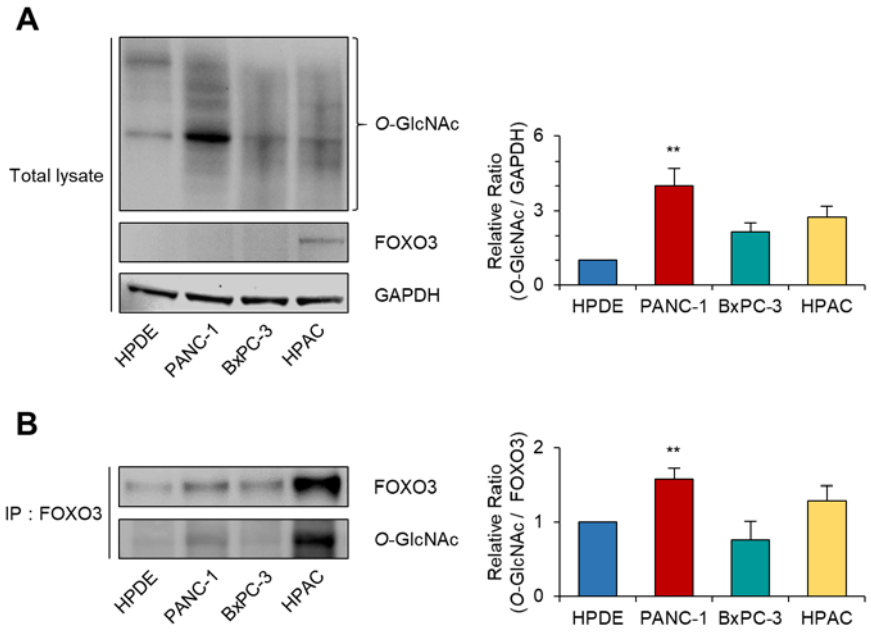
A
Total lysate
O-GlcNAc
FOXO3
GAPDH
HPDE
PANC-1
BxPC-3
HPAC
Relative Ratio (O-GlcNAc / GAPDH)
6
3
0
**
HPDE
PANC-1
BxPC-3
HPAC
B
IP : FOXO3
FOXO3
O-GlcNAc
HPDE
PANC-1
BxPC-3
HPAC
Relative Ratio (O-GlcNAc / FOXO3)
2
1
0
**
HPDE
PANC-1
BxPC-3
HPAC

Figure S2

A

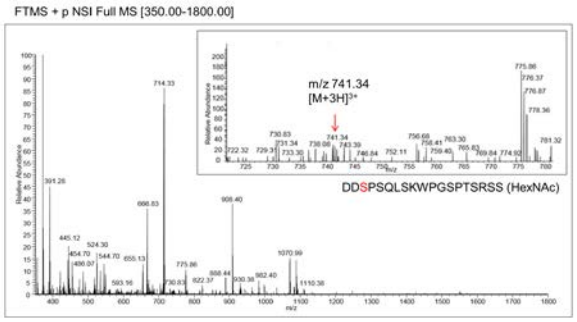

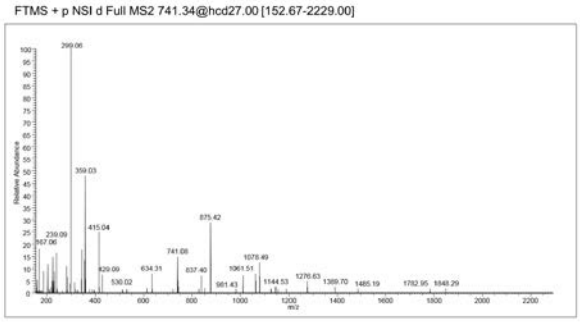

B

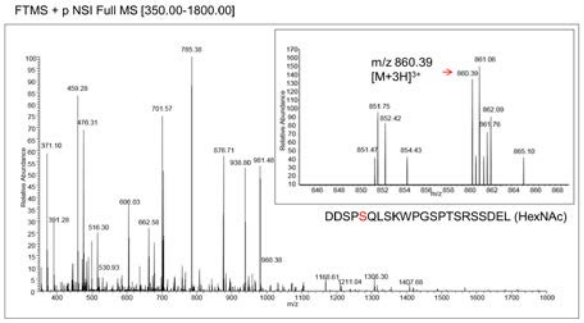

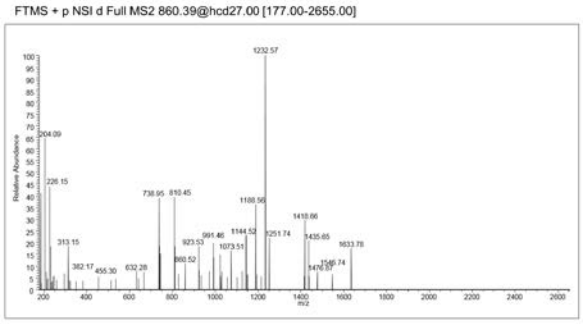

C

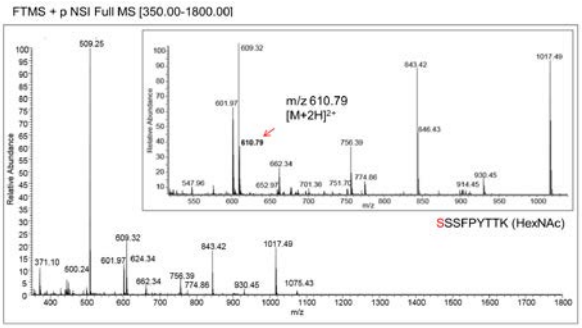

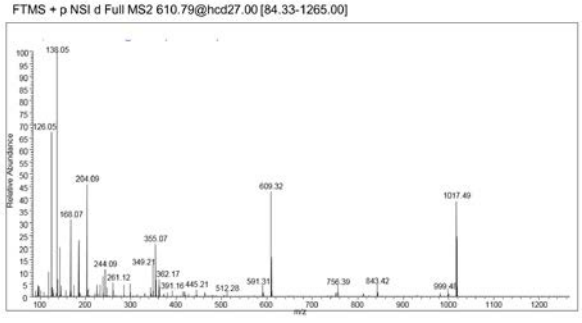

D

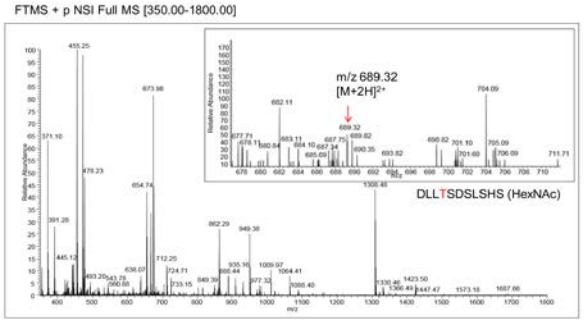

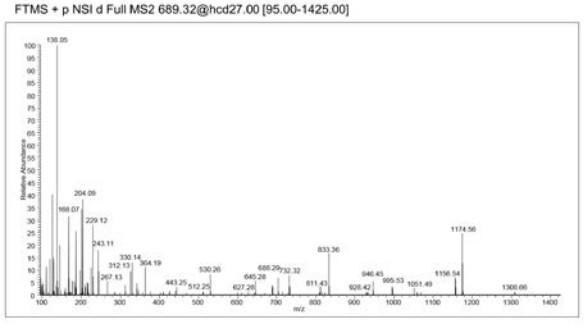

Figure S2

E

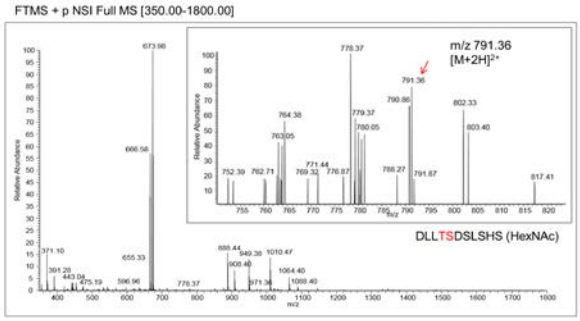

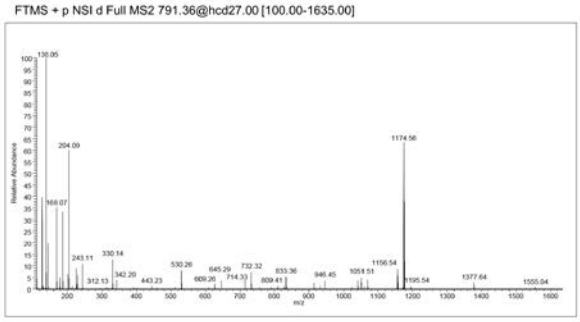

F

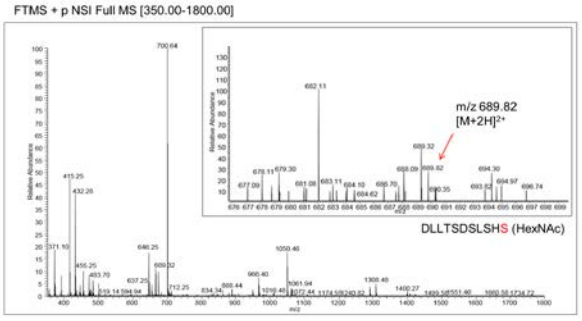

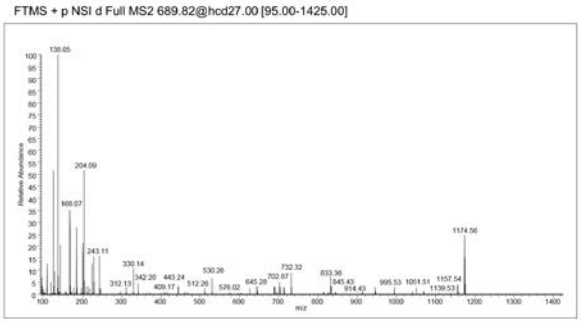

G

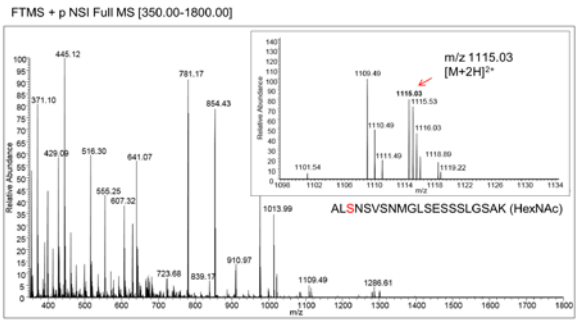

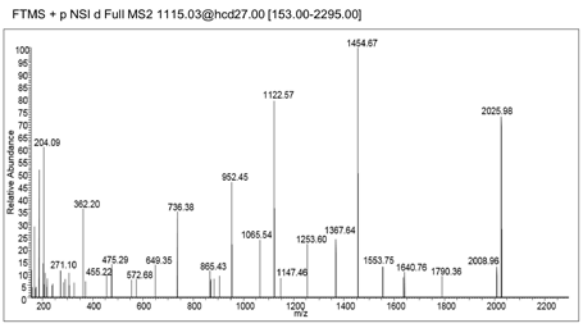

Figure S3

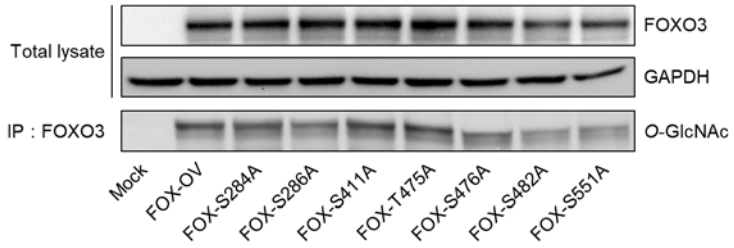
Total lysate
FOXO3
GAPDH
IP : FOXO3
O-GlcNAc
Mock
FOX-OV
FOX-S284A
FOX-S286A
FOX-S411A
FOX-T475A
FOX-S476A
FOX-S482A
FOX-S551A

Figure S4

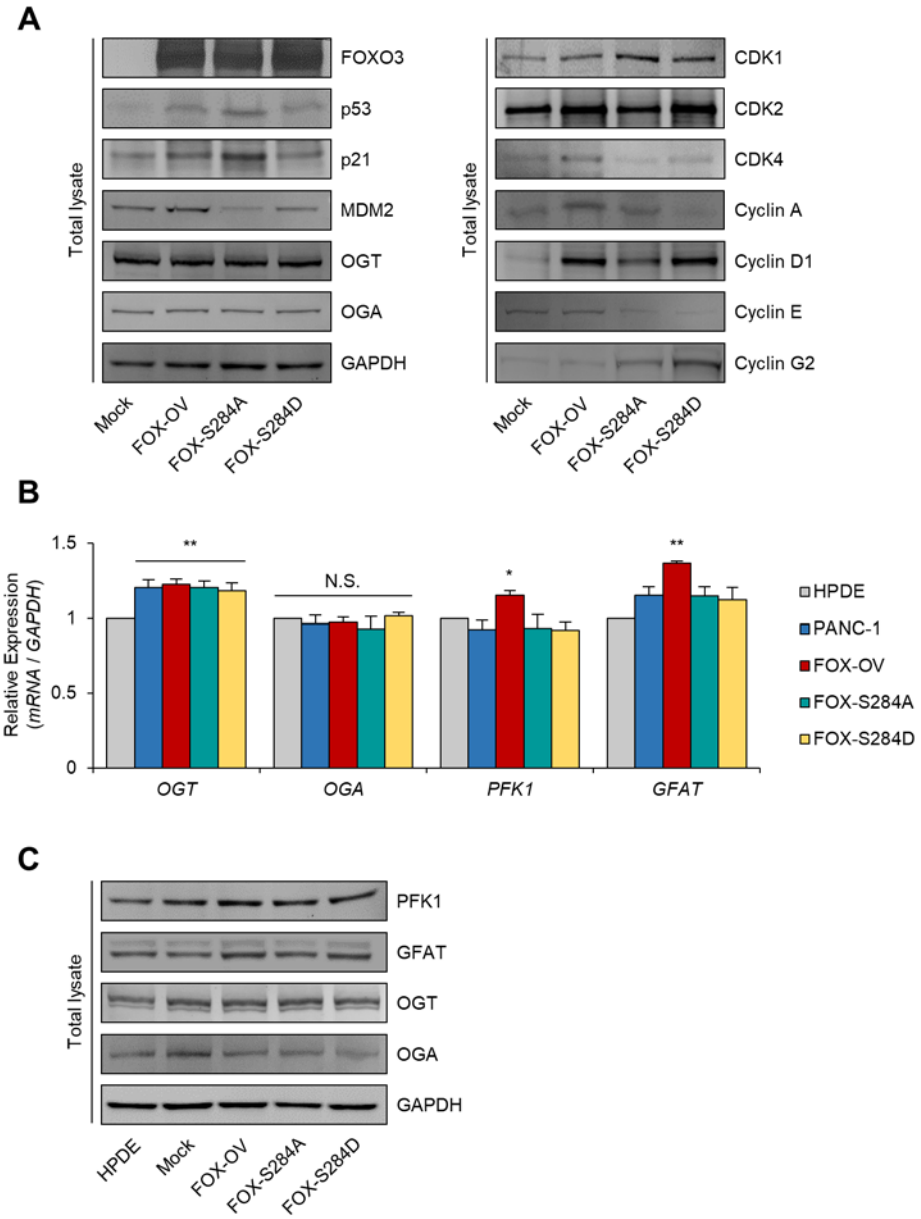
A
Total lysate
FOXO3
p53
p21
MDM2
OGT
OGA
GAPDH
Mock
FOX-OV
FOX-S284A
FOX-S284D
Total lysate
CDK1
CDK2
CDK4
Cyclin A
Cyclin D1
Cyclin E
Cyclin G2
Mock
FOX-OV
FOX-S284A
FOX-S284D
B
Relative Expression
(mRNA / GAPDH)
1.5
1
0.5
0
**
N.S.
*
**
OGT
OGA
PFK1
GFAT
HPDE
PANC-1
FOX-OV
FOX-S284A
FOX-S284D
C
Total lysate
PFK1
GFAT
OGT
OGA
GAPDH
HPDE
Mock
FOX-OV
FOX-S284A
FOX-S284D

Figure S5

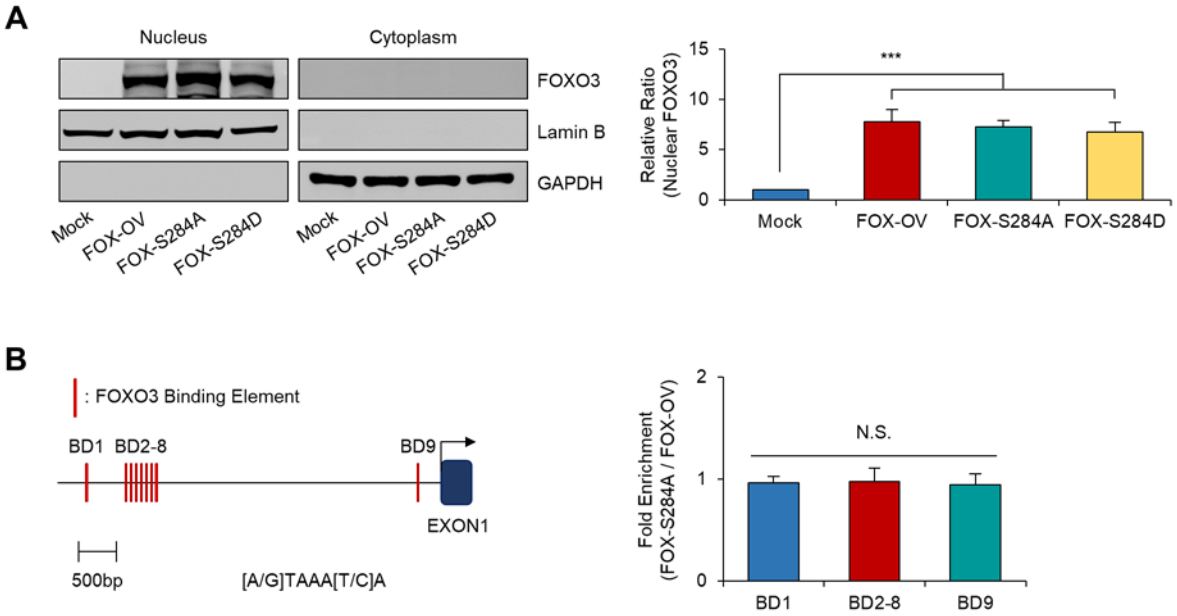
A
Nucleus
Cytoplasm
FOXO3
Lamin B
GAPDH
Mock
FOX-OV
FOX-S284A
FOX-S284D
Mock
FOX-OV
FOX-S284A
FOX-S284D
Relative Ratio (Nuclear FOXO3)
15
10
5
0
***
Mock
FOX-OV
FOX-S284A
FOX-S284D
B
: FOXO3 Binding Element
BD1
BD2-8
BD9
EXON1
500bp
[A/G]TAAA[T/C]A
Fold Enrichment (FOX-S284A / FOX-OV)
2
1
0
N.S.
BD1
BD2-8
BD9